

## Holographic Imaging of Atoms Using Multiple-Wave-Number Electron Angular Distribution Patterns

L. J. Terminello

*Lawrence Livermore National Laboratory, Livermore, California 94550*

J. J. Barton and D. A. Lapiano-Smith

*IBM Thomas J. Watson Research Center, P.O. Box 218, Yorktown Heights, New York 10598*

(Received 20 January 1992)

We have imaged Cu atoms near a (100) single-crystal face using photoelectron holography and have applied for the first time a multiple-wave-number method for improving the quality of images obtained from experimental results. When compared to images obtained from single-energy holograms, the structural information extracted from the multiple-wave-number, phased-sum method gives substantial resolution improvement, twin-image suppression, and artifact reduction.

PACS numbers: 61.14.-x, 42.40.Ht

First suggested by Szöke [1], and subsequently formalized by Barton [2], the holographic imaging of atoms using coherent electron emission from solids has been demonstrated experimentally [3–5]. The angular distribution of localized electron emission from atoms in an ordered solid constitute an electron hologram, and from this hologram, scattering-atom images can be numerically reconstructed [2,6,7]. Ideally, these scattering-atom images constitute a direct determination of the crystallographic structure surrounding the electron-emitting site.

In both experimental [3–5] and theoretical [8–10] work, the quality of images generated by Fourier inversion of the electron angular distribution patterns is degraded by the presence of spurious artifacts, multiple scattering, and equal-intensity conjugate (twin) images, in addition to distortion of the atom images themselves. Several methods have been developed to improve the quality of electron-holographic images. Scattering amplitude- and phase-compensation schemes have succeeded in reducing the atom-position distortions of hologram reconstructions [11,12], but they require *a priori* knowledge of what is being investigated (i.e.,  $Z$ -dependent scattering factors) to improve the quality of the image. Restricted-windowing methods require, in addition, estimates of the atomic positions [9]. However, the multiple-wave-number transform method proposed by Barton [6,13] suppresses twin-image and multiple-scattering artifacts using only experimentally obtainable information (the hologram and its measured energy). Here we demonstrate the efficacy of multiple-wave-number holography on a simple experimental system, the Cu  $3p$  photoelectron holograms measured from a Cu(001) bulk surface.

Cu(001) surfaces were prepared according to well established cleaning and annealing procedures [14]. Valence-band photoemission was used to orient the electron emission directions with respect to the analyzer, and all photoelectron spectra were measured using an ellipsoidal mirror analyzer that has been described previously [15]. This band-pass electron-energy analyzer can mea-

sure both angle-resolved and angle-integrated spectra, permitting both characterization of the sample (angle-integrated) and measurement of the  $3p$  photoelectron holograms (angle-resolved).

Our measurements were conducted on the IBM U8 beam line [16] at the National Synchrotron Light Source which provided the 316–560 eV photons needed for this experiment. Copper  $3p$  electron angular distributions of  $82^\circ$  full-angle acceptance were measured at nine kinetic energies ranging from 244 to 477 eV as indicated in Fig. 1. This energy range does not yield as high a resolution image as much shorter-wavelength electrons have provided [3], because the diffraction-limited resolution parallel to the crystal face is  $0.51 \text{ \AA}$  for our analyzer at 477 eV, compared to  $0.34 \text{ \AA}$  at 1075 eV. However, this range had several experimental advantages: The cross section for Cu  $3p$  photoemission in this energy range is well matched with the flux throughput of the monochromator, giving high photoelectron yields, and non-forward-scattering intensities are at a maximum (but still smaller than forward scattering intensities) in this region of  $k$  space, thereby illuminating atoms below the emitter as well as those above [17]. Thus, the hopes of observing back-scattering atoms in systems other than bulk materials may be realized through this choice of energy range.

To isolate the holographic interference information from the raw electron angular distribution patterns, a simple two-dimensional background removal was used for each energy. These techniques are similar to those used for energy-dependent photoelectron diffraction [14]. The ellipsoidal mirror electron analyzer used in this experiment introduced an angular distortion to the measured electron angular distribution pattern that was removed by a polynomial image-transform algorithm [18]. The oscillatory portion of our holograms was isolated by removing a background that was created by convoluting a low-pass filter with the experimental hologram. This background removal scheme also tends to eliminate the strong forward peak upon which the structure-containing interference fringes reside [8]. This improved image quality by

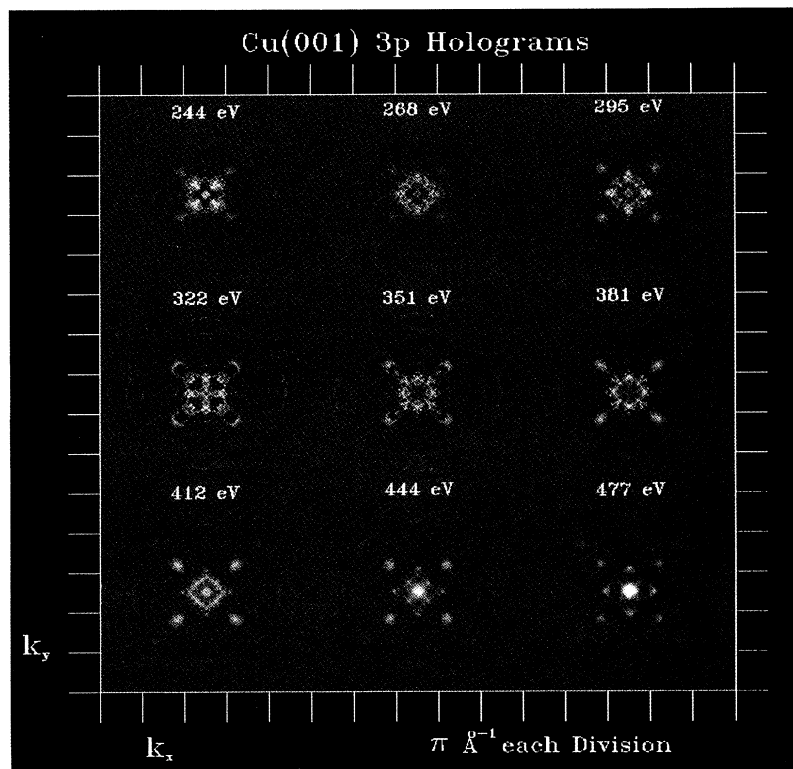


FIG. 1. Each panel is the fourfold, symmetry-averaged hologram extracted from the Cu 3*p* photoelectron angular distribution. The scale for each  $k_x$  and  $k_y$  hologram is  $\pi \text{ \AA}^{-1}$  per division and each frame has the kinetic energy indicated. Each hologram has been multiplied by a Gaussian window and appears just as it would prior to Fourier transformation. The full range of intensity for the thermal color scale (the same as in Fig. 2) is  $-0.10$  to  $0.20$ .

eliminating reconstruction artifacts. Each hologram was fourfold symmetry averaged, and was then multiplied by a Gaussian window to reduce Fourier truncation errors. All nine holograms are pictured in Fig. 1 and were Fourier transformed according to the algorithm developed by Barton [2].

To render the structural information in an objective manner and view the entire reconstruction simultaneously, we have chosen to present three-dimensional isosurfaces through the volume. An example of this volume-contouring method is shown in panel A of Fig. 2, which is a rendering of spheres representing the Cu atoms surrounding a near-surface 3*p* emitter.

One image (at 477 eV) of the nine we measured in this work is shown in panel B of Fig. 2 at a contour level of 60% of maximum; note the strong twin image below the plane of the emitter and the high-intensity artifacts residing within that plane. Nonetheless, assignment of intensity maxima to scattering atoms is possible. The atomic-resolution image created from the 477-eV hologram shown in Fig. 1 renders the nearest-neighbor atoms with approximately  $\frac{1}{2} \text{ \AA}$  resolution but shifted away from the emitter by  $0.5 \text{ \AA}$ . We can attribute this shift from the actual scattering-atom position to the additional phase incurred during the scattering process [3–5]. This compares well with earlier experimentally derived holographic atom images in spite of the lower energy that we have used to achieve greater lateral atom sensitivity.

Phase-summed images of the Cu 3*p* photoelectron holograms were created using the multiple-wave-number transform proposed and demonstrated by Barton [13]. Briefly, this approximation can be described as

$$M(\mathbf{r}) = \sum_i F_i(k_i, \chi_i, \mathbf{r}) e^{-ik_i r}, \quad (1)$$

where the resultant real-space ( $\mathbf{r}$ ) scattering-atom amplitude  $M(\mathbf{r})$  is given by a sum over the individual reconstructed holograms  $F_i(k_i, \chi_i, \mathbf{r})$ —which were computed from the holograms  $\chi_i(k_i)$  measured at each wave vector  $k_i$ —times  $\exp(-ik_i r)$ , the phase term that isolates the real, single-scattering contribution to the reconstruction. Twin images are suppressed because their phase dependence as a function of wave number has opposite sign from that of the true image. The absolute value of the complex term  $M(\mathbf{r})$  gives a three-dimensional power spectrum in  $\mathbf{r}$  space that has intensity maxima located near scattering-atom positions. The result of the nine-energy phased sum is shown in panel C of Fig. 2 with a contour level of 70% of maximum. The atoms visible in the isodensity rendering of panel C are indicated in Fig. 2, panel E as atoms 1 and 2. Figure 2, inset D is a two-dimensional slice through the multiple-wave-number Fourier volume in panel C taken through the four first-layer atoms directly above the electron emitter. The four scattering atoms are the highest intensity features in the image slice, and the suppression of artifacts is evident from the low intensity in the center of the cut.

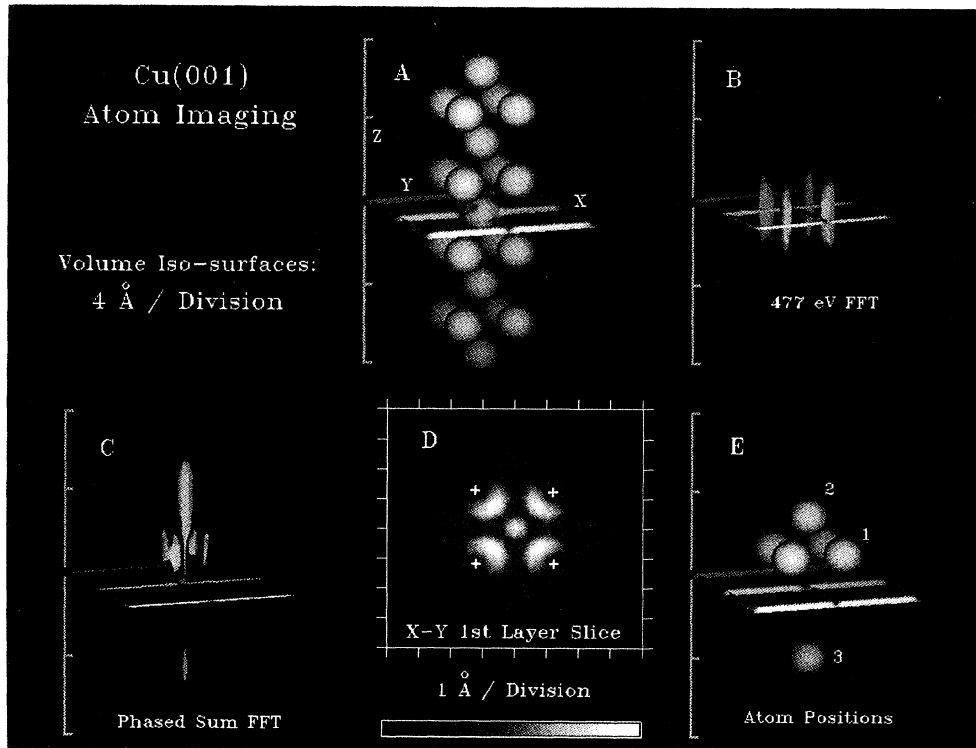


FIG. 2. Panel A is a volume-contour rendering of the atoms within a copper single-crystal lattice. This columnar slice is a schematic to indicate the Cu atom positions that are near a given emitter. The Cu atoms are superimposed on a  $8 \times 8 \text{ \AA}$  plane which is parallel to the Cu(001) surface but intersects the electron emitting atom (located at the center of the plane). A vertical scale parallel to the surface normal has  $4 \text{ \AA}$  markings to aid in the  $z$  direction interpretation. The Fourier transform of the Cu  $3p$  477-eV hologram is shown volume-contour rendered in panel B; again, a reference plane and scale is inserted into the volume to help provide perspective. Panel C is a similar three-dimensional rendering of the holographically derived intensity information but is obtained from the phased sum of the nine energy hologram transforms. The inset D is a slice parallel to the Cu(001) surface taken through the first layer of atoms above the reference plane in panel C. Each division in the inset D is  $1 \text{ \AA}$ , and the plus signs indicate the actual atom positions for the first-layer atoms. Panel E depicts the atoms (forward-scattering atoms 1 and 2) near the emitter (at the center of the reference plane) that are visible in the panel C volume rendering.

We note that for the multiple-wave-number, phased-summing method, the conjugate image that is prominent in single-energy transforms has been mostly eliminated. Some aspects of conjugate image suppression have been achieved by scattering factor compensation methods, but they unfortunately require *a priori* knowledge of which scattering factors to use. Our background removal approach reduces many of the artifacts present in the atom reconstructions; however, the multiple-wave-number method further improves the final image by suppressing the emitter-plane artifacts seen in the single-energy reconstruction (Fig. 2, panel B).

Scattering atoms appear shifted from their nominal lattice location in the multiple-wave-number (Fig. 2, panel C) and single-energy (Fig. 2, panel B) images [3,8,19]. As mentioned earlier, atom position distortions owing to the additional phase introduced by the scattering physics have been observed in earlier experimental electron holography studies [3] and also in Fourier-transformed, energy-dependent, photoelectron diffraction [20,21]. For

our multiple-wave-number, phase-summed image, we obtain a radial shift from the actual atom position of  $0.4 \text{ \AA}$  towards the emitter for the first-layer atoms (atoms 1, Fig. 2, panel E), and at  $0.9 \text{ \AA}$  shift for the second-layer atom located directly above the emitter (atom 2, Fig. 2, panel E). We noted earlier that the 477-eV single-energy hologram produced a first-layer atom image (Fig. 2, panels C and D) shifted away from the actual atom position (by  $0.5 \text{ \AA}$ )—opposite in direction from the emitter than the phase-summed atom image. We can deduce that this translation of first-layer atom image can be attributable to variations as a function of energy in the Cu scattering phase shifts [22]. In fact, this trend is observable in the series of atom reconstructions (not pictured) made from our nine holograms and because of the impact on holographic imaging fidelity, merits further study. Figure 2, panels B and C have slightly different contour levels merely for enhancing the visualization of the phased-sum result, and no alteration of our conclusions occurs when the contour levels are varied, or kept the

same.

The forward-scattering atoms imaged in this experiment are a combination of near-surface and bulk atoms because of the depth-sampling limitations (electron mean free path) in our kinetic energy range. It is not surprising that atoms which lie between the emitter and the detector dominate the Fourier reconstruction because forward-scattering amplitudes dominate over backscattering intensities throughout the structurally useful range of wave numbers. However, within the energy range that we selected for our multiple-wave-number treatment, electron backscattering intensities have been calculated to be within a factor of 10 of forward-scattering intensities [17]. Moreover, it is important to note that in our multiple-wave-number atom rendering, the twin-image intensity is 10 times smaller than the true image. Thus, our results suggest that the remaining intensity below the emitter plane of Fig. 2, panel C may be attributed to a combination of the true image of a backscattering atom (atom 3, Fig. 2, panel E), because of the symmetry of the lattice, and the remaining twin image of the forward scatterer (atom 2, Fig. 2, panel E), even though it has been suppressed. However, holographic atom imaging from an adsorbate overlayer on a single-crystal surface would be a clearer demonstration of imaging backscattering atoms.

In conclusion, we have demonstrated for the first time that the atom imaging capabilities of experimental photoelectron holography can be improved by implementing the multiple-wave-number, phase-summed approximation suggested by Barton [13]. This method of image enhancement requires nothing more than the measured electron angular distribution patterns from a solid sample and their respective energies. Our results using the multiple-wave-number summing approximation have shown significant artifact and conjugate-image suppression with experimental multiple-wave-number holograms. Furthermore, we have observed sufficient twin-image suppression so that contributions from backscattering atoms to the resultant image may be observable with selection of an appropriate experimental system. This result, taken with the improved image quality that phased summing provides, suggests that less trivial adsorbate systems and buried interfaces can be successfully imaged with photoelectron holography. While having to measure several different kinetic-energy holograms may appear to restrict the method, it is clear that some means of conjugate-image suppression for these self-referencing holograms is needed to successfully image buried hetero-interfaces. For a system of unknown constituency, the multiple-wave-number, phase-summing method would be eventually a desirable holographic imaging aid because it only requires the experimental observables—the holograms and their energies—as input.

We would like to thank C. Costas and J. Yurkas for technical assistance with the experiment. This work was conducted under the auspices of the U.S. Department of

Energy by the Lawrence Livermore National Laboratory under Contract No. W-7405-ENG-48, and was conducted at the National Synchrotron Light Source, Brookhaven National Laboratory, which is supported by the Department of Energy (Division of Materials Sciences and Division of Chemical Sciences of Basic Energy Sciences) under Contract No. DE-AC02-76CH0016.

- 
- [1] A. Szöke, in *Short Wavelength Coherent Radiation: Generation and Applications*, edited by D. T. Attwood and J. Bokor, AIP Conf. Proc. No. 147 (American Institute of Physics, New York, 1986).
  - [2] J. J. Barton, *Phys. Rev. Lett.* **61**, 1356 (1988).
  - [3] G. R. Harp, D. K. Saldin, and B. P. Tonner, *Phys. Rev. Lett.* **65**, 1012 (1990).
  - [4] Z. L. Han, S. Hardcastle, G. R. Harp, H. Li, X. D. Wang, J. Zhang, and B. P. Tonner, *Surf. Sci.* **258**, 313 (1991).
  - [5] G. S. Herman, S. Thevuthasan, T. T. Tran, Y. J. Kim, and C. S. Fadley, *Phys. Rev. Lett.* **68**, 650 (1992).
  - [6] J. J. Barton and L. J. Terminello, in "Structure of Surfaces III," edited by S. Y. Tong, M. A. Van Hove, X. Xide, and K. Takayanagi (Springer-Verlag, Berlin, to be published).
  - [7] D. K. Saldin, G. R. Harp, B. L. Chen, and B. P. Tonner, *Phys. Rev. B* **44**, 2480 (1991).
  - [8] S. Thevuthasan, G. S. Herman, A. P. Kaduwela, R. S. Saiki, Y. J. Kim, and C. S. Fadley, *Phys. Rev. Lett.* **67**, 469 (1991).
  - [9] H. Huang, Hua Li, and S. Y. Tong, *Phys. Rev. B* **44**, 3240 (1991).
  - [10] C. M. Wei, T. C. Zhao, and S. Y. Tong, *Phys. Rev. Lett.* **65**, 2278 (1990).
  - [11] B. P. Tonner, Zhi-Lan Han, G. R. Harp, and D. K. Saldin, *Phys. Rev. B* **43**, 14423 (1991).
  - [12] S. Y. Tong, C. M. Wei, T. C. Zhao, H. Huang, and Hua Li, *Phys. Rev. Lett.* **66**, 60 (1991).
  - [13] J. J. Barton, *Phys. Rev. Lett.* **67**, 3106 (1991).
  - [14] C. C. Bahr, J. J. Barton, Z. Hussain, S. W. Robey, J. G. Tobin, and D. A. Shirley, *Phys. Rev. B* **35**, 3773 (1987).
  - [15] D. E. Eastman, J. J. Donelon, N. C. Hien, and F. J. Himpsel, *Nucl. Instrum. Methods* **172**, 327 (1980).
  - [16] F. J. Himpsel, Y. Jugnet, D. E. Eastman, J. J. Donelon, D. Grimm, G. Landgren, A. Marx, J. F. Morar, C. Oden, R. A. Pollack, J. Schneir, and C. Crider, *Nucl. Instrum. Methods Phys. Res.* **222**, 107 (1984).
  - [17] J. J. Barton and D. A. Shirley, *Phys. Rev. B* **32**, 1892 (1985).
  - [18] L. J. Terminello and J. J. Barton (to be published).
  - [19] D. Hardcastle, Z.-L. Han, G. R. Harp, J. Zhang, B. L. Chen, D. K. Saldin, and B. P. Tonner, *Surf. Sci.* **245**, L190 (1991).
  - [20] J. J. Barton, C. C. Bahr, S. W. Robey, Z. Hussain, E. Umbach, and D. A. Shirley, *Phys. Rev. B* **34**, 3807 (1986).
  - [21] L. J. Terminello, X. S. Zhang, Z. Q. Huang, S. H. Kim, A. E. Schach von Wittenau, K. T. Leung, and D. A. Shirley, *Phys. Rev. B* **38**, 3879 (1988).
  - [22] J. J. Barton, Z. Hussain, and D. A. Shirley, *Phys. Rev. B* **35**, 933 (1987).

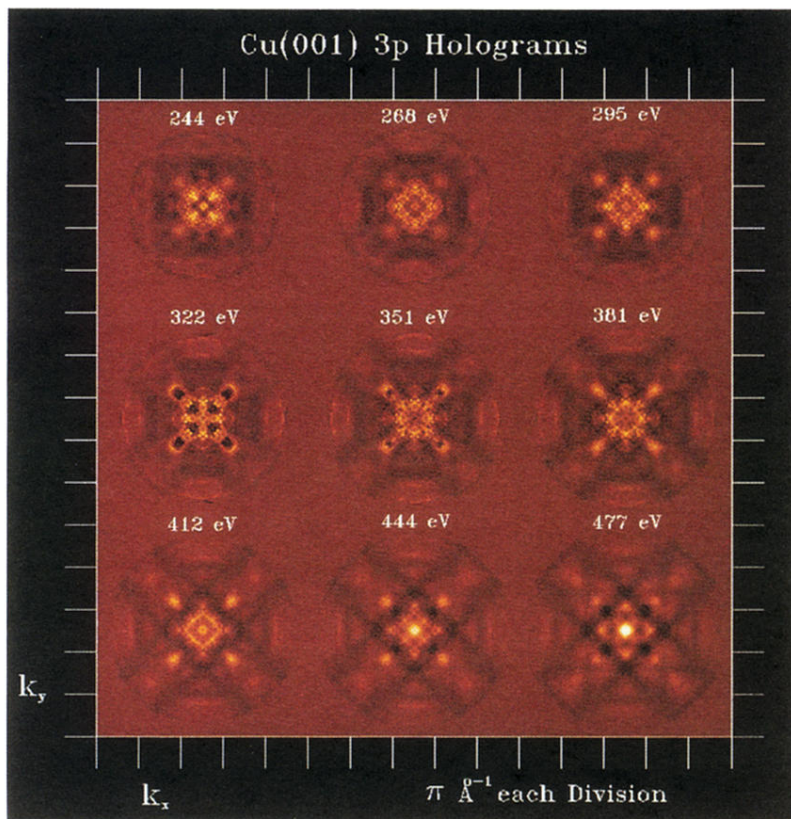


FIG. 1. Each panel is the fourfold, symmetry-averaged hologram extracted from the Cu 3p photoelectron angular distribution. The scale for each  $k_x$  and  $k_y$  hologram is  $\pi \text{ \AA}^{-1}$  per division and each frame has the kinetic energy indicated. Each hologram has been multiplied by a Gaussian window and appears just as it would prior to Fourier transformation. The full range of intensity for the thermal color scale (the same as in Fig. 2) is  $-0.10$  to  $0.20$ .

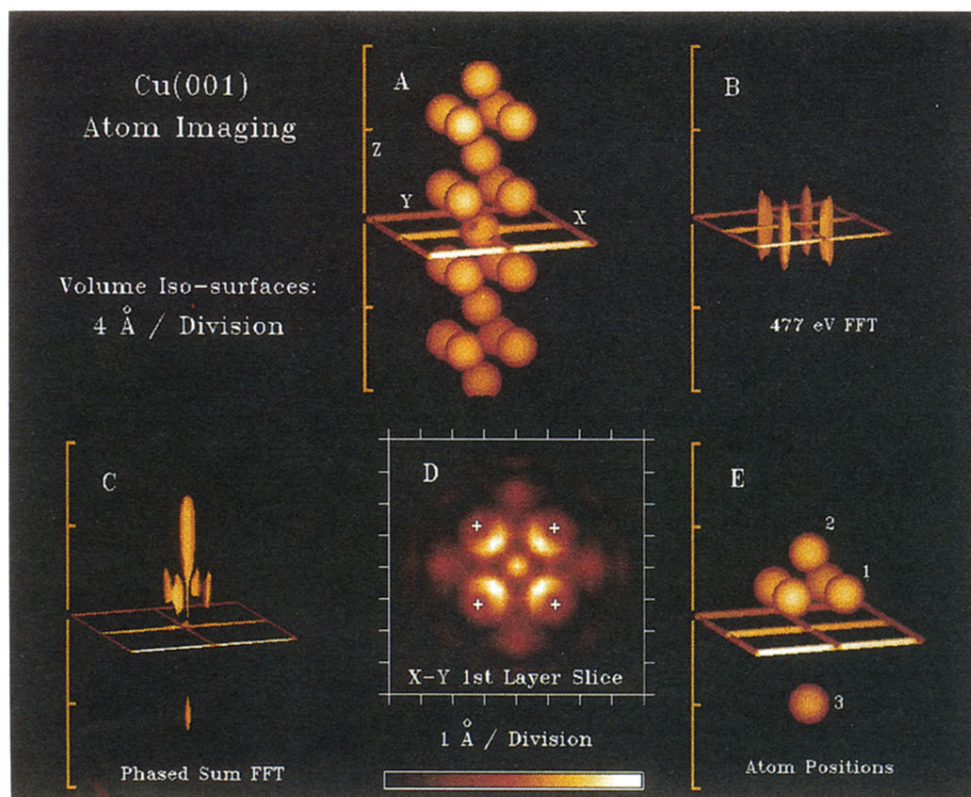


FIG. 2. Panel A is a volume-contour rendering of the atoms within a copper single-crystal lattice. This columnar slice is a schematic to indicate the Cu atom positions that are near a given emitter. The Cu atoms are superimposed on a  $8 \times 8 \text{ \AA}$  plane which is parallel to the Cu(001) surface but intersects the electron emitting atom (located at the center of the plane). A vertical scale parallel to the surface normal has  $4 \text{ \AA}$  markings to aid in the  $z$  direction interpretation. The Fourier transform of the Cu  $3p$  477-eV hologram is shown volume-contour rendered in panel B; again, a reference plane and scale is inserted into the volume to help provide perspective. Panel C is a similar three-dimensional rendering of the holographically derived intensity information but is obtained from the phased sum of the nine energy hologram transforms. The inset D is a slice parallel to the Cu(001) surface taken through the first layer of atoms above the reference plane in panel C. Each division in the inset D is  $1 \text{ \AA}$ , and the plus signs indicate the actual atom positions for the first-layer atoms. Panel E depicts the atoms (forward-scattering atoms 1 and 2) near the emitter (at the center of the reference plane) that are visible in the panel C volume rendering.